Electronic Supplementary Information

Experimental Section

Synthesis of *c*-Bi/CF: The *c*-Bi NAs/CF was synthesized based on our previous research, with minor modifications[1]. Typically, 316 mg of $BiCl_3$ was dissolved in 50 mL of DMSO solution. The Cu foam was cut into 1×2 cm^2, immersed into HCl (3 M) for cleaning. Then wash with deionized water and ethanol alternately for three times. The cleaned Cu foam was immersed into the above solution allowed to stand at room temperature for 24 h. The final product was collected, and washed thoroughly with water and ethanol alternately three times. The sample is vacuum dried overnight at 50 ℃.

Synthesis of *a*-BiB/CF: The synthesis of method for *a*-BiB NAs/CF is similar to that of *a*/*c*-BiB NAs/CF, but 3.0 mg DMAB was dissolved in 5 mL of DMSO solution to form solution B.

Synthesis of Ni-MOF/NF: The Ni-MOF/NF was synthesized based on our previous research, with minor modifications[2]. Firstly, 0.3 g of $NiN_2O_6 \cdot 6H_2O$, 0.033 g of TED and 0.105 g of PTA were added into 30 mL DMF to form a transparent green solution by ultrasonic dissolution. A nickel foam (2×4 cm^2) was ultrasonically cleaned with dilute HCl (3 M) for 15 minutes. Then the mixed solution and the cleaned Ni foam were placed in a 50 mL Teflon-lined autoclave and heated at 130 °C for 14 hours. Finally, it was naturally cooled to room temperature, and the nickel foam was taken out and washed with ethanol for many times, and dried overnight at 50 °C to obtain Ni-MOF/NF.

Synthesis of NiO/CN/NF: The pre-synthesized Ni-MOF/NF (2×4 cm^2) was transferred to a porcelain ship and heated to 350 °C at a heating rate of 10 °C min^{-1} in an air atmosphere, and maintained at 350 °C for 4 hours before cooling to room temperature to obtain NiO/CN/NF.

Characterizations

Scanning electron microscopy (SEM) images were obtained on a ZEISS Gemini 500 apparatus, along with the energy-dispersive X-ray spectroscopy (EDX) analysis. The mesoporous structure of the catalysts was determined using a transmission electron microscope (TEM) (JEOL-2010) operated at 200 kV. X-ray photoelectron spectroscopy (XPS) analysis was carried out on microprobe spectrometer (ULVAC PHI Quantera) with Al-Kα radiation. X-ray diffraction (XRD) pattern was performed on D8 ADVANCE (Bruker AXS, Germany). Gas chromatograph equipped with thermal conductivity detector and helium ionization detector (GC-2014) was used to analyze gas products (H_2 and CO). The liquid products were analyzed by Bruker AVANCE III HD spectrometer during the electrolysis. Inductively coupled plasma-optical emission spectrometry (ICP-OER) analysis was performed on Agilent ICPOES730.

Electrochemical measurements

All electrochemical experiments were performed in a H-type gas cell, and the two chambers are separated with proton exchange membrane. Each chamber contained 30 mL electrolyte (0.5 M $KHCO_3$) with gas headspace of 20 mL. Cu foam loaded with bismuth-based catalyst (1×1 cm^2), Pt foil (1×1 cm^2) and Ag/AgCl electrodes (saturated KCl solution) were used as the working electrode, counter electrode and reference electrode, respectively. All potentials are converted to RHE reference standards, by use *E* (*vs*. RHE) =*E* (*vs*. Ag/AgCl) +0.197 V+ 0.0591 V× pH. Before the electrochemical test, the electrolyte was used to bubble at least 30 min with CO_2, to ensure CO_2 saturation is kept in the entire test (pH=7.8). By quality flow controller, the CO_2 gas enters the H-type gas tight cell at a speed of 20 mL min^{-1}. The electrochemical workstation (CHI 660E) controls the potential at the normal temperature and normal pressure. Linear scanning voltammetry (LSV) measurement was performed in the Ar or CO_2-saturated 0.5 M $KHCO_3$ with a scan rate of 10 mV s^{-1}. The Bruker AVANCE III HD nuclear magnetic resonance was used to analyze the liquid products

after electrolysis. The internal standard solution contained 5 μL (0.1408 mM) dimethyl sulfoxide (DMSO) and 95 μL D_2O. Then 0.5 mL $KHCO_3$ solution containing the liquid product was mixed with 0.1 mL internal standard solution by ultrasonication before measurement. The liquid products were quantified by ^1H NMR with solvent (H_2O) suppression. The ^1H spectrum peak of formate is ~8.3, ^1H spectrum peak of DMSO is ~2.6.

The MOR and OER electrochemical activities of the catalysts were evaluated on a CHI 660E electrochemical workstation. The prepared NiO/CN/NF was cut into 1×1 cm^2 as the working electrode by using a conventional three-electrode system : carbon rod, Ag/AgCl electrode as the counter electrode and reference electrode, respectively. The current density of OER and MOR is normalized to the geometric area of the nickel foam substrate, according to the Nernst equation (*E* (*vs*. RHE) = *E* (*vs*. Ag/AgCl) +0.197 V+ 0.0591 V× pH). The linear sweep voltammetry (LSV) curve was tested in 1 M KOH and 1 M methanol (5 mV s^{-1}). Based on the excellent catalytic activity and selectivity of NiO/CN/NF for methanol oxidation and *a*/*c*-BiB NAs/CF for CO_2 reduction to formate, a two-electrode electrolytic cell was constructed using the anode and cathode, respectively. The cathodic electrolyte was 30 mL CO_2-saturated 0.5 M $KHCO_3$ and the anodic electrolyte was 30 mL Ar-saturated 1 M KOH containing 1 M methanol**.**

Faradaic efficiency (FE) calculation:

Electrocatalytic carbon dioxide reduction:

The Faradaic efficiency were calculated using the following formula[3, 4]:

$$FE\ (\%) = \frac{Q^-(product)}{Q^-\ (total)} \times 100\% = \frac{n \times F \times N_{product}{}^-}{I \times t} 100\%$$

where the Q^-(product) represents the charge quantity for H_2, HCOOH and CO. The Q^-(total) represents the total charge quantity during the entire cathodic reduction.

n: the number of transfer electrons.

F: the Faraday constant (96485 C mol $^{-1}$).

$N^{-}_{product}$: the mole number of the product, which was quantified by means of the standard curve line of GC and Ion chromatography.

I: the practical test current density at a constant potential (A s^{-1}).

t: the reaction time (s).

Electrocatalytic methanol oxidation:

$$FE = \frac{N \times Z \times F}{Q} \times 100\%$$

N : the mole of product (H_2 or formate) produced.

Q : the passed charge.

F : the Faraday constant (96,485 C mol^{-1}).

Z : the number of formate (Z = 4) formation.

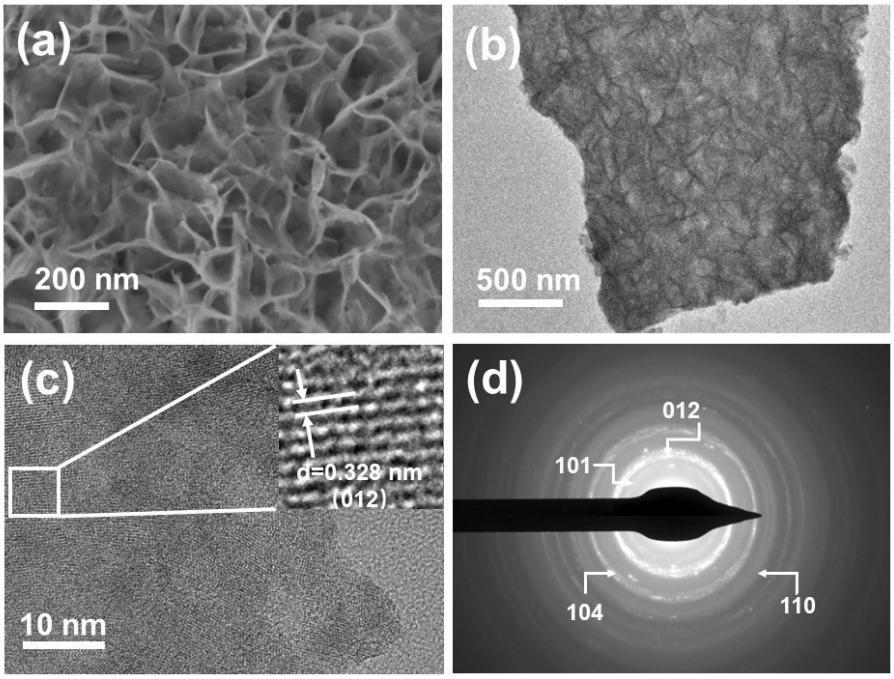

Fig. S1 (a) SEM image of *c*-Bi NAs/CF. (b)TEM image of *c*-Bi nanosheets. (c)HRTEM image of *c*-Bi nanosheets. (d) SAED pattern of *c*-Bi nanosheets.

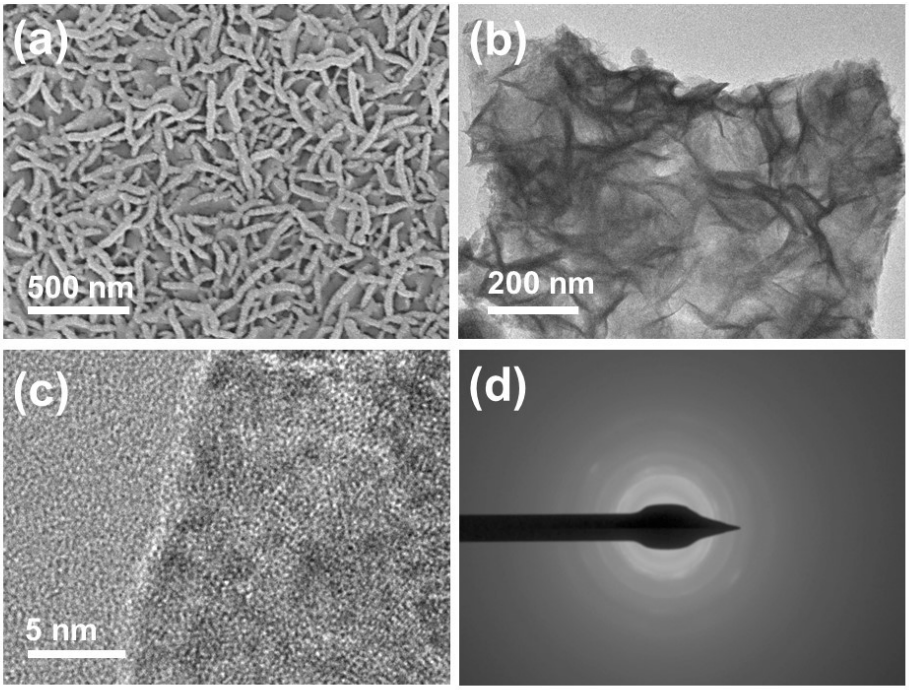

Fig. S2 (a) SEM image of *a*-BiB NAs/CF. (b) TEM image of *a*-BiB nanosheets. (c) HRTEM image of *a*-BiB nanosheets. (d) SAED pattern of *a*-BiB nanosheets.

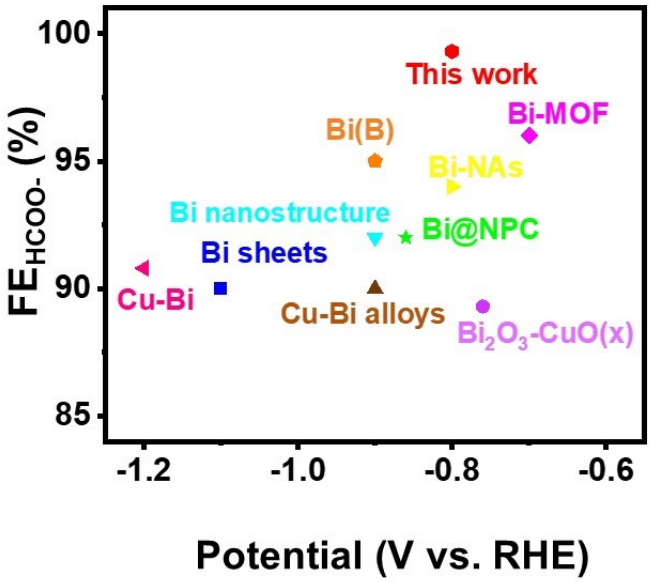

Fig. S3 Comparison of FE_{HCOO-} and applied potential of *a*/*c*-BiB nanosheets and some recently reported Bi-based catalysts towards CO_2RR.

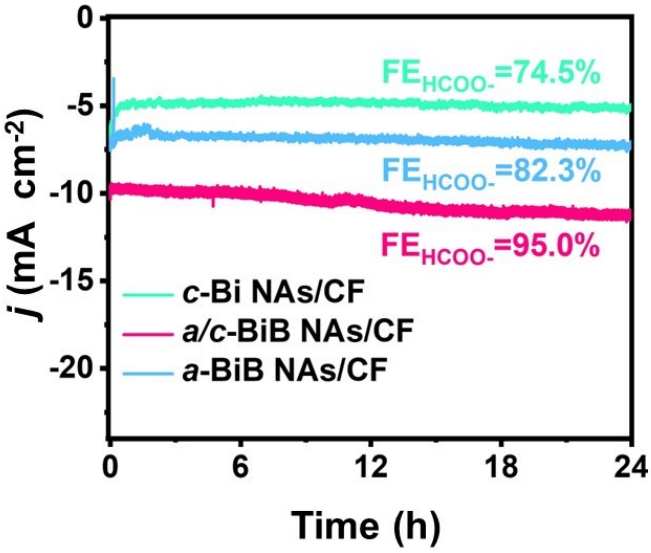

Fig. S4 Stability test for *c*-Bi NAs/CF, *a*/*c*-BiB NAs/CF and *a*-BiB NAs/CF at -0.8 V vs. RHE.

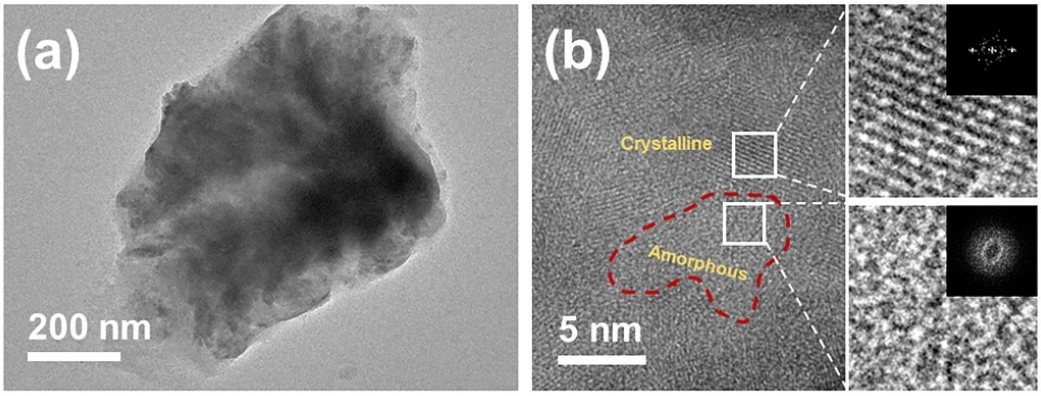

Fig. S5 (a) TEM image and (b) HRTEM image of the post-tested *a*/*c*-BiB nanosheets.

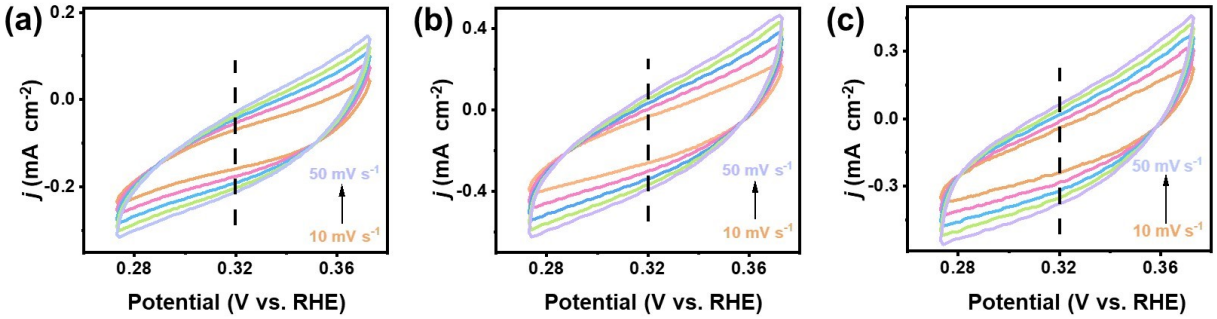

Fig. S6 Electrochemical double-layer capacitance measurements of (a) *c*-Bi NAs/CF, (b) *a*/*c*-BiB NAs/CF and (c) *a*-BiB NAs/CF in a 0.5 M $KHCO_3$ solution.

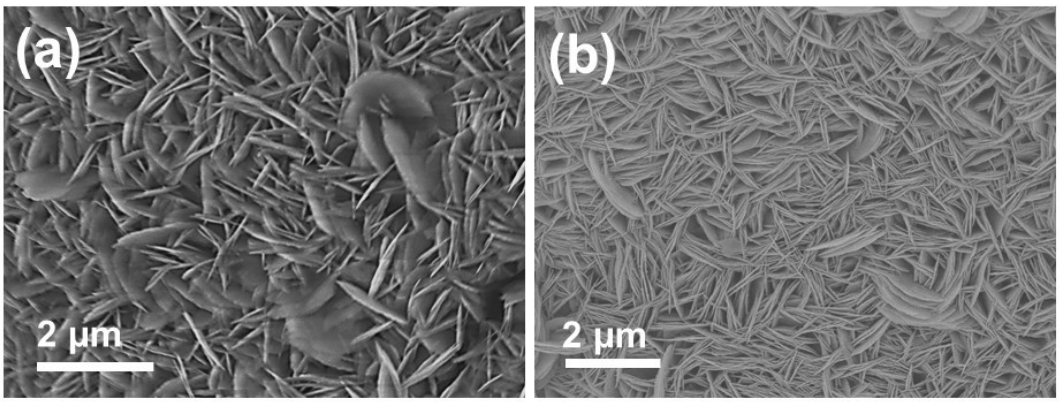

Fig. S7 SEM images of (a) Ni-MOF/NF and (b) NiO/CN/NF.

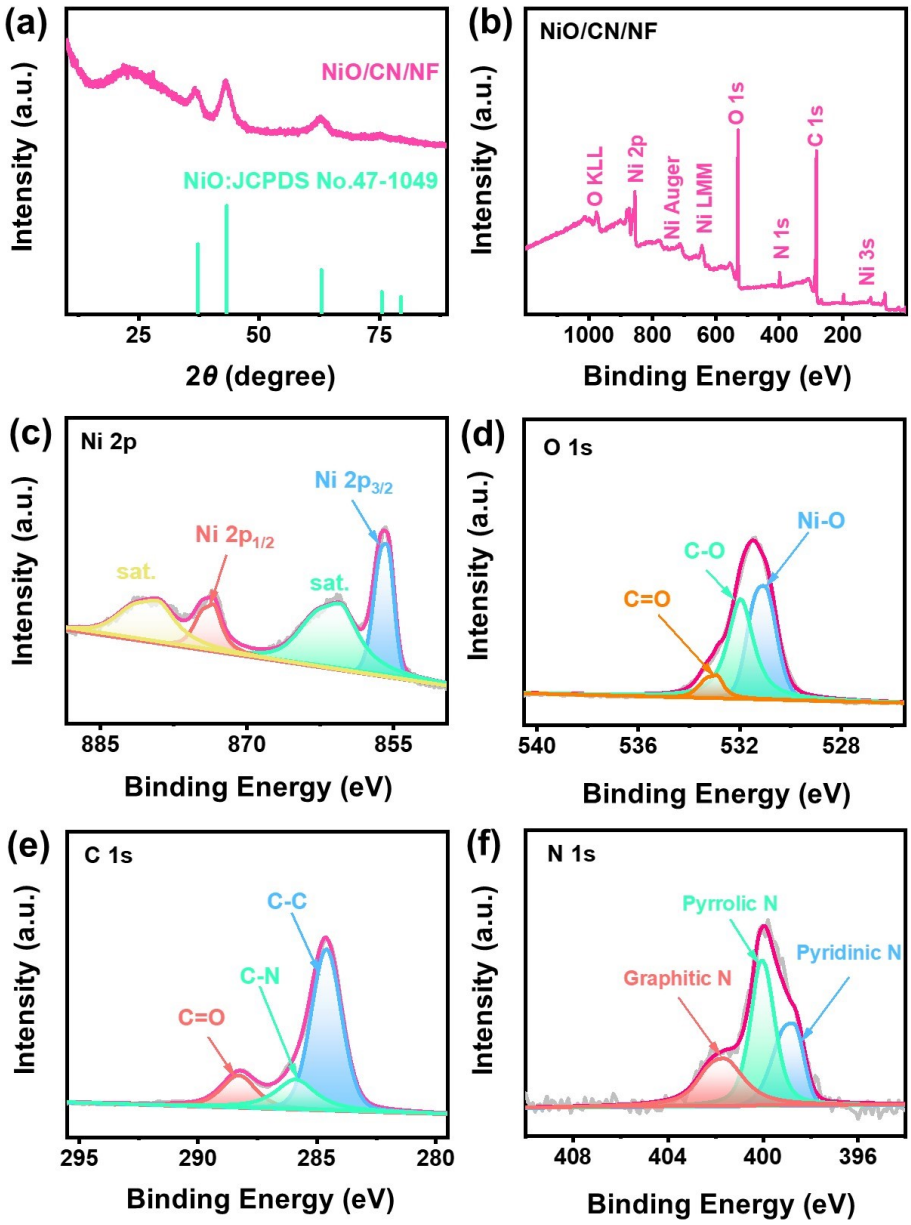

Fig. S8 (a) XRD pattern of the NiO/CN/NF. (b) XPS survey spectrum of NiO/CN/NF. High-resolution XPS spectra of Ni 2p (c), O 1s (d), C 1s (e) and N 1s (f) for the NiO/CN/NF.

Table S1 The atomic ratio of Bi and B, and loading amount of Bi for various samples.

Catalysts	Atomic ratio of Bi (%)	Atomic ratio of B (%)	Loading amount of Bi (mg cm^2)
c-Bi NAs/CF	100	0	2.69
***a/c*-BiB NAs/CF**	**54**	**46**	**2.56**
a-BiB NAs/CF	36	64	2.55

Table S2 Comparison of max FE_{HCOO^-} for various catalysts.

Catalysts	**Max FE_{HCOO^-} (Applied potential)**
c-Bi NAs/CF	83.8 (-0.9 V vs. RHE)
***a/c*-BiB NAs/CF**	**99.3** (-0.8 V vs. RHE)
a-BiB NAs/CF	89.6 (-0.7 V vs. RHE)

Table S3 Comparison of FE_{HCOO-} and applied potential of *a*/*c*-BiB nanosheets and some recently reported Bi-based catalysts towards CO_2RR.

Catalysts	Electrolyte	Applied Potential	FE_{HCOO-} (%)	Reference
***a/c*-BiB NAs/CF**	**0.5 M $KHCO_3$**	**-0.8 V (vs. RHE)**	**99.3**	**This work**
Bi-NAs	0.5 M $KHCO_3$	-0.8 V (vs. RHE)	94.0	1
Cu-Bi	0.5 M $KHCO_3$	-1.2 V (vs. RHE)	90.8	5
Bi(B)	0.1 M $KHCO_3$	-0.9 V (vs. RHE)	95.0	6
Bi nanostructure	0.5 M $KHCO_3$	-0.9 V (vs. RHE)	92.0	7
Cu–Bi alloys	0.1 M $KHCO_3$	-0.9 V (vs. RHE)	90.0	8
Bi@NPC	0.1 M $KHCO_3$	-1.5 V (vs. SCE)	92.0	9
Bi_2O_3-$CuO_{(x)}$	0.5 M $KHCO_3$	-1.4 V (vs. SCE)	89.3	10
Bi-MOF	0.5 M $NaHCO_3$	-0.7 V (vs. RHE)	96.0	11
Bi_2S_3	0.1 M $KHCO_3$	-1.1 V (vs. RHE)	90.0	12

References

1. J. Fan, X. Zhao, X. Mao, J. Xu, N. Han, H. Yang, B. Pan, Y. Li, L. Wang and Y. Li, *Adv. Mater.*, 2021, **33**, e2100910.
2. Y. Xu, M. Liu, M. Wang, T. Ren, K. Ren, Z. Wang, X. Li, L. Wang and H. Wang, *Appl. Catal. B: Environ.*, 2022, **300**, 120753.
3. Y. Sheng, Y. Guo, H. Yu, K. Deng, Z. Wang, X. Li, H. Wang, L. Wang and Y. Xu, *Small*, 2023, **19**, e2207305.
4. Y. Xu, Y. Guo, Y. Sheng, H. Yu, K. Deng, Z. Wang, X. Li, H. Wang and L. Wang, *Small*, 2023, DOI: 10.1002/smll.202300001, e2300001.
5. M. Y. Zu, L. Zhang, C. Wang, L. R. Zheng and H. G. Yang, *J. Mater. Chem. A*, 2018, **6**, 16804-16809.
6. X. Chen, H. Chen, W. Zhou, Q. Zhang, Z. Yang, Z. Li, F. Yang, D. Wang, J. Ye and L. Liu, *Small*, 2021, **17**, e2101128.
7. P. Lu, D. Gao, H. He, Q. Wang, Z. Liu, S. Dipazir, M. Yuan, W. Zu and G. Zhang, *Nanoscale*, 2019, **11**, 7805-7812.
8. Z. B. Hoffman, T. S. Gray, Y. Xu, Q. Lin, T. B. Gunnoe and G. Zangari, *ChemSusChem*, 2019, **12**, 231-239.
9. D. Zhang, Z. Tao, F. Feng, B. He, W. Zhou, J. Sun, J. Xu, Q. Wang and L. Zhao, *Electrochimica Acta*, 2020, **334**, 135563.
10. C. Dai, Y. Qiu, Y. He, Q. Zhang, R. Liu, J. Du and C. Tao, *New J. Chem*, 2019, **43**, 3493-3499.
11. C. Cao, D. D. Ma, J. Jia, Q. Xu, X. T. Wu and Q. L. Zhu, *Adv. Mater.*, 2021, **33**, e2008631.
12. P. F. Sui, C. Xu, M. N. Zhu, S. Liu, Q. Liu and J. L. Luo, *Small*, 2022, **18**, e2105682.